

Progress on the application of ELM control schemes to ITER scenarios from the non-active phase to DT operation

A. Loarte¹, G. Huijsmans¹, S. Futatani¹, D.J. Campbell¹, T. Casper¹, E. Daly¹, Y. Gribov¹, R.A. Pitts¹, S. Lisgo¹, A. Sashala Naik¹, L.R. Baylor², T.E. Evans³, D. M. Orlov⁴, A. Wingen², O. Schmitz⁵, H. Frerichs⁵, A. Kischner⁵, R. Laengner⁵, G. Saibene⁶, M. Becoulet⁷, P. Cahyna⁸, A. Kavin⁹

¹ITER Organization, Route de Vinon sur Verdon, 13115 Saint Paul lez Durance, France

²Oak Ridge National Laboratory, Oak Ridge, Tennessee 37831, USA

³General Atomics, P.O. Box 85608, San Diego, California 92186-5608, USA

⁴University of California-San Diego, La Jolla, California 92093, USA

⁵Forschungszentrum Jülich GmbH, Association EURATOM-FZJ, 52428 Jülich, Germany

⁶Fusion for Energy Joint Undertaking, c/ Josep Pla, n° 2, 08019 Barcelona, Spain

⁷CEA/IRFM, Cadarache, 13108 St Paul-lez-Durance Cedex – France

⁸Institute for Plasma Physics AS CR, Za Slovankou 3, 182 00 Prague 8, Czech Republic

⁹Efremov Research Institute, Metallostroy, 196641 Saint-Petersburg, Russia

E-mail contact of main author: alberto.loarte@iter.org

Abstract. Progress in the definition of the requirements for ELM control and the application of ELM control methods both for high fusion performance DT operation and non-active low current operation in ITER is described. Uncontrolled ELMs for low plasma current H-modes are not likely to lead to damage to the W divertor target. Despite this, some level of ELM control is expected to be required in ITER to prevent an excessive contamination of the plasma by W which could eventually lead to an increased disruptivity. Progress on the determination of the physics processes determining the flow of energy from the confined plasma onto the plasma facing components during ELMs at the ITER scale and on the triggering of ELMs by pellet injection with the non-linear MHD code JOREK are described. The evaluation of the capabilities of the ELM control coil system in ITER for ELM suppression (in the vacuum approximation) is presented as well as the consequences for the spatial distribution of the power fluxes at the divertor. The feasibility of the use of the in-vessel vertical stability coils for ELM control in low plasma current H-modes in ITER is described.

1. Introduction

High fusion performance DT operation (inductive, hybrid and steady-state) in ITER is based on the achievement of the H-mode confinement regime with $H_{98} \geq 1$ and an edge transport barrier that is expected to lead to the quasi-periodic triggering of ELMs. Operation of ITER with H-mode plasmas is also foreseen during the non-active (H & He) and DD operation allowing the development of ELM control schemes before DT operation [1]. Naturally occurring (or “uncontrolled”) ELMs in ITER are expected to lead to large power fluxes to plasma facing components (PFCs) which can decrease significantly their lifetime. In order to ensure an appropriate lifetime of ITER PFCs, guidance for the maximum power fluxes on these components has been set to avoid localised melting of the edges of the individual macro-brushes in the W divertor and Beryllium first wall plasma facing components. This maximum power limit corresponds to 50% of the energy density required to melt the front face of these components, which are in direct contact with the plasma in stationary phases [2]. These material limits combined with the spatial and temporal characteristics of the ELM power fluxes expected in ITER on the basis of present experimental results and modelling are then used to evaluate the maximum ELM energy losses which would meet the PFC lifetime requirements in ITER (so-called controlled ELMs). The evaluation of the maximum energy loss for controlled ELMs is carried out for a range of plasma conditions and compared to that expected for uncontrolled ELMs in the same conditions. A major issue that remains to be understood in order to have such sound evaluation is that of the area over which the ELM energy is deposited. Present experimental evidence indicates that the area for ELM energy deposition at the divertor can be significantly larger than that between ELMs and that it depends on the magnitude of the ELM energy loss [3, 4]. A larger effective area for ELM divertor power flux allows a larger total ELM energy loss from the main plasma to be acceptable while avoiding divertor damage. However, this could also lead to increased ELM energy fluxes to the wall, if the same transport mechanisms broaden the ELM divertor footprint also broaden the ELM power flux width in the main chamber. Assuming that this is the case, the limitations to ELM energy losses imposed avoiding damage of both the W divertor and the Be wall can be evaluated as shown in Fig. 1. It is important to note that the evaluation shown in Fig. 1 includes not only assumptions on the broadening of the ELM

power flux footprint at the inner and outer divertors (assumed to be the same) but also on other important key parameters determining the magnitude of the divertor target ELM power flux deposition : the timescale for ELM energy deposition (determined by the ion parallel transport timescale in agreement with experiments), the SOL power flux width between ELMs ($\lambda_p \sim I_p^{-1}$ with $\lambda_p(15 \text{ MA}) = 5 \text{ mm}$) and the in/out ELM energy deposition asymmetry (2:1 in agreement with experimental results). For small ELM broadening the limit to the ELM energy loss for controlled ELMs is set by the W divertor while for larger broadening the limit is set by the Be wall. Based on this evaluation, ELM energy losses during the initial operation of ITER in the non-active He/H phase (which is expected to involve plasma currents up to 7.5MA) [1] are not foreseen to pose a major risk to the PFCs and thus ELM control requirements to avoid damage are rather modest in this phase; i.e., a controlled decrease of a factor of 2 or less (depending on broadening assumptions) of the ELM energy loss from that of uncontrolled ELMs would be required. Thus, in the non-active phase the need for ELM control will be dominated by the avoidance of W in the main plasma, which will be produced

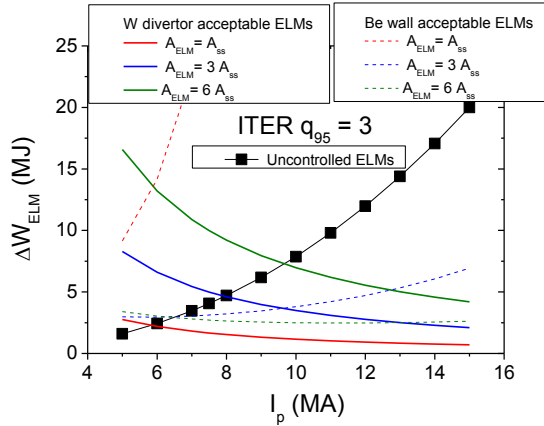


Figure 1. Limits to the acceptable ELM energy loss (ΔW_{ELM}) for the W divertor and the Be first wall for ITER H-modes versus plasma current for various assumptions regarding the broadening of the ELM power flux width (a midplane separatrix-wall distance of 5 cm, an average of 10 filaments per ELM and an average angle of incidence of 70° for the field line on the wall are assumed).

evaluating the expected W divertor influxes in ITER (between ELMs and at the ELMs). For the extrapolation of the effective W divertor shielding to ITER, the physics guidelines derived from ASDEX-Upgrade [5] have been applied; the effective shielding is assumed to increase with the transport time of W from the divertor target into the pedestal plasma and to decrease with increasing ELM repetition time (i.e. decreasing ELM frequency). Unlike present experiments in which W transport in the SOL dominates the W penetration timescales, transport of W through the pedestal is expected to dominate in ITER. This is due to the scaling of neoclassical transport which is found to describe appropriately W behaviour between ELMs and which is very low at the ITER scale [5] ($v_{pinch-pedestal}^W = 1.8 \text{ ms}^{-1}$ requiring 33ms to travel through the $\sim 6 \text{ cm}$ pedestal plasma in ITER to be compared with ASDEX-Upgrade $v_{pinch-pedestal}^W = 90 \text{ ms}^{-1}$ requiring 0.2ms to travel through the $\sim 1.5 \text{ cm}$ pedestal plasma). As shown in Fig. 2.a, although uncontrolled ELMs with a broadening of 3 may be acceptable from the W divertor damage point of view, the expected low ELM frequencies of such ELMs (few Hz's) at low currents ($I_p \leq 8 \text{ MA}$) may be insufficient to prevent a significant edge W concentration ($\sim 10^{-4}$) of these low current H-modes. Although recent results from ASDEX-Upgrade with strong electron heating have demonstrated that it is possible to sustain good H-mode performance for similar core W levels [8], termination of the H-mode and, possibly, even disruptions in ITER cannot be excluded at such high W levels. In this regard, the range of ELM frequencies at which W accumulation is expected to become problematic in ITER is similar to that observed in present experiments at JET and ASDEX-Upgrade in which serious W accumulation is found for ELM frequencies such that $f_{ELM} \times \tau_E \leq 5-10$ [5, 6]. Application of this simple model to evaluate the requirements for the control of W concentration in ITER indicates that an ELM frequency in the range of 10 - 20 Hz should be sufficient to maintain this concentration at the $2.5 \cdot 10^{-5}$ level, as shown in Fig. 2.b; this corresponds to a product of $f_{ELM} \times \tau_E \sim 25-40$.

by physical sputtering of the divertor between and at the ELMs. Present experimental evidence in tokamaks operating with W components shows that W produced by plasma-wall interactions accumulate at the edge of the confined plasma between ELMs and is effectively expelled by ELMs. Thus a minimum ELM frequency is required to prevent W accumulation to occur in the main plasma which can lead to the loss of the H-mode and in some cases to a disruption [5, 6]. An initial evaluation of these requirements for ITER (to be refined by advanced modelling in the near future), has been carried out by extrapolating present experimental results of the effective W divertor shielding in ASDEX-Upgrade [7] and

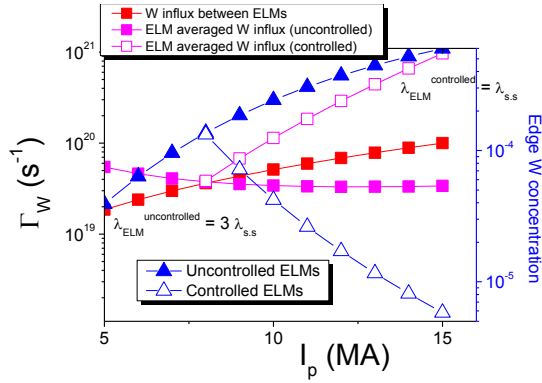


Figure 2.a. Expected W divertor fluxes between and during the ELMs in ITER for uncontrolled and controlled ELMs ($P_{ELM} = 0.3 P_{SOL}$ and $\Delta N_{ELM}/N_{tot} = 2.5\%$) and resulting edge W concentration.

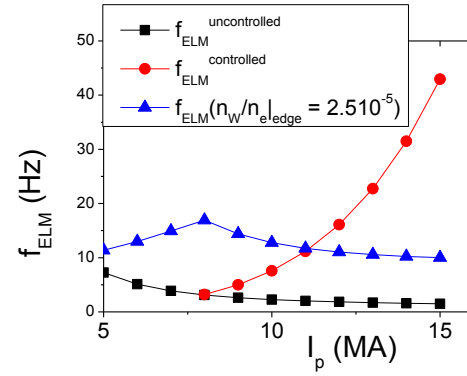


Figure 2.b. Expected ELM frequency for uncontrolled and controlled ELMs in ITER and required ELM frequency to maintain an edge W concentration of $2.5 \cdot 10^{-5}$.

In order to advance the understanding of the ELM characteristics and their control in ITER plasmas a two-pronged approach is thus followed: one involves the experimental/theoretical research at the ITER members' tokamak facilities through their own programmes and that coordinated under the ITPA activities and the other the application of the models developed and, as far as possible, validated against the experimental results to the ITER plasma conditions. This paper provides an overview of progress in the latter set of activities, which are described in more detail in accompanying papers at this conference [9, 10, 11, 12].

2. Non-linear MHD modelling of ELM power fluxes in ITER.

In order to improve understanding of the ELM energy fluxes to PFCs, non-linear simulations of the ELM crash in ITER have been carried out with the JOEKE non-linear MHD code which includes the transport of energy from the main plasma onto the divertor and wall PFCs [9]. Simulations have been carried out for the 15 MA $Q_{DT} = 10$ plasma conditions. So far relatively small ELM energy losses for the ITER scale (1.5 - 4 MJ) have been obtained, which are much smaller than those expected from empirical scaling to ITER for these plasma conditions (~ 20 MJ) [2]. Despite this, the simulations have provided key insight on the physics mechanisms that are responsible for transport of energy from the main plasma to PFCs at the ITER scale and on their influence on the magnitude and spatial characteristic of the ELM fluxes. For the case with an ELM energy loss of 4 MJ, it is found that the non-linear growth of the MHD activity during the ELM crash creates an ergodic layer at the plasma edge (reminiscent of that obtained with edge magnetic field perturbations) leading to a direct connection between the divertor and the confined plasma and to a large conductive heat flux along these ergodised field lines (i.e. ELM losses are dominated by conduction). On the contrary, for the smaller ELMs (~ 1.5 MJ) the level of edge ergodization is much smaller and energy is lost from the confined plasma by the growth and expulsion of plasma filaments with little change to the plasma temperature (i.e. convective ELMs). Despite the different ELM energy transport mechanisms and the different detailed shapes of the divertor ELM power flux profiles (see Fig. 3), the effective area for energy deposition at the outer divertor are similar (within a factor of 1.5) for both ELM simulations [9]. This corresponds to an effective "e-folding length" for the ELM heat flux of 1.5 - 2.0 cm mapped to the outer midplane, i.e., a broadening of 3 - 4 when compared to the effective power e-folding of ~ 5 mm expected between ELMs at 15 MA. Such broadening would increase the controlled ELM size for these conditions in ITER from 0.7 MJ to 2.1-2.8 MJ. Contrary to the divertor targets, in which the dominant mechanism for ELM energy deposition changes with ELM type : parallel conduction in the ergodised edge for larger ELMs versus energy loss along the "intact" (i.e. as in between ELMs) poloidal field from detached filaments for smaller ELMs, the mechanism for ELM energy transport to the first wall is the same for the range of ELM energy losses simulated so far. This is the convection of energy in the radially propagating filaments. JOEKE simulations show that its magnitude does not depend on the size of the ELM energy loss. The proportion of ELM energy deposited at the wall is $\sim 10\%$ for ~ 1.5 MJ ELM but only $\sim 4\%$ for the 4 MJ ELM. These modelling results indicate that the ELM power fluxes to the first wall in ITER are not related in a straightforward way to the total ELM energy loss

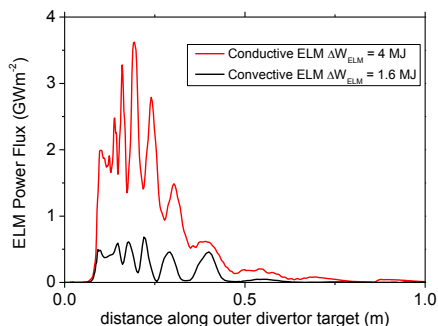


Figure 3. Peak ELM power flux for a 4 MJ conductive and a 1.6 MJ convective ELM versus distance along the outer divertor target.

progress in the refinement of the evaluation of the maximum tolerable ELMs in ITER shown in Fig. 1; namely the sharing of the ELM energy flux between the inner and outer divertor targets and the broadening of the inner divertor footprint during the ELM.

3. Modelling of controlled ELM triggering by pellet injection.

Control of the ELM frequency and ELM energy loss by the injection of pellets is one of the two main ELM control schemes planned foreseen in ITER, which has been investigated thoroughly in several tokamaks (ASDEX-Upgrade, JET and DIII-D). Recently, DIII-D has demonstrated the very high capabilities of this technique to reduce the ELM energy deposited at the divertor. These DIII-D experimental results have achieved a reduction of the ELM energy deposited at the divertor by a factor of ~ 20 for controlled ELMs by pellet injection compared to uncontrolled ones for the same discharge conditions, i.e. an ITER-relevant range [13]. Important issues that need to be addressed regarding the application of this technique to ITER include: the required pellet size to reliably trigger ELMs (which has implications for the fuel throughput associated with this technique), the adequacy of the ITER pellet injection geometry (in the low field side of the plasma above the X-point) for ELM triggering, possible toroidal asymmetries of divertor power for pellet triggered ELMs, and impact on the pedestal and core plasma parameters.

Modelling of ELM triggering by pellet injection has been performed with the non-linear code JOREK which has been upgraded to include an appropriate description of the pellet ablation physics [10]. Before applying this model to ITER, its predictions have been compared with experiments in DIII-D in which ELMs have been triggered by injection of pellets at the outer midplane and above the X-point with ITER-like injection geometry [13]. JOREK simulations show that triggering of ELMs by pellet injection is caused by the large toroidally-localised edge pressure gradients produced by the pellet. When these gradients exceed a threshold, ballooning modes grow non-linearly leading to the ELM crash. Exceeding this pressure gradient threshold implies that, for given pedestal plasma conditions, a minimum pellet size is required to trigger an ELM. JOREK modelling shows that this minimum pellet size depends on the injection geometry and that for injection above the X-point the required pellet size in DIII-D is a factor of ~ 2 smaller than for midplane injection, as shown in Figs. 4.a and 4.b [10]. This indicates that the ITER pellet injection geometry for ELM control is advantageous to reduce the fuel throughput requirements associated with this ELM control scheme. Modelling of the divertor power flux for pellet triggered ELMs in DIII-D shows that this has a sizeable non-toroidally symmetric peak (i.e. of similar magnitude to the separatrix strike point ELM power flux) away from the separatrix (3-4 cm) at the outer divertor target, which has also been observed at JET [14]. This secondary peak has $n = 1$ symmetry and it is caused by the expulsion of a plasma filament in the vicinity of the pellet injection location that takes with it a large fraction of the pellet injected particles.

Application of the JOREK model for pellet triggering of ELMs to ITER has proven to be very numerically challenging. This is due to the large edge temperatures expected in ITER, which lead to a large ablation rate of the pellet as soon as it enters the plasma and to the formation of very steep density profiles near the separatrix. The results of the scans carried out so far indicate that a pellet size of $\sim 34 \text{ mm}^3$ with an injection velocity of 350m/s is required for the triggering of ELMs in 15 MA $Q_{DT} = 10$ plasmas [10]. This is well within the proposed

and to the effective broadening of the ELM divertor footprint, as assumed in the simplified model used to derive Fig. 1. Indeed these modelling results challenge the appropriateness of the direct extrapolation of the empirical picture to the ITER scale [3, 4] that relates the divertor ELM power deposition area to the magnitude of the ELM energy loss and/or the peak ELM divertor power flux to the pedestal plasma parameters [3]. Further work is required, and is in progress, to compare in detail the predictions of the JOREK code against experiments with emphasis on two aspects that are key to the

capabilities of the pellet injector in ITER [15] but implies that a sizeable proportion of the fuel throughput ($\sim 50\%$) may be required by this technique of ELM control for $Q_{DT} = 10$ scenarios.

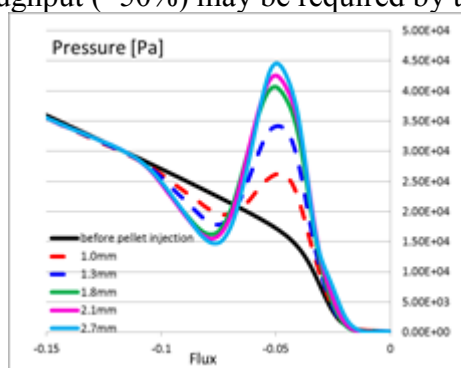


Figure 4.a. Modelled pressure perturbations at the time of ELM triggering in DIII-D for midplane injection. Dashed lines correspond to the maximum pressure for pellet sizes which do not trigger ELMs.

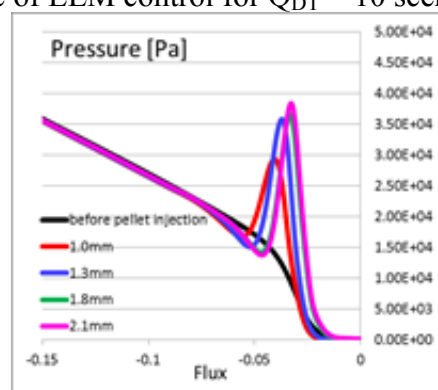


Figure 4.b. Modelled pressure perturbations at the time of ELM triggering in DIII-D for injection in the X-point region.

4. Application of edge magnetic field perturbations for ELM control in ITER.

Control of ELMs by edge magnetic field perturbations is the second main ELM control scheme foreseen in ITER. For this purpose, a set of 27 in-vessel coils (above, below and at the midplane) are considered for ITER with a maximum current carrying capability of 90 kA-turns [16]. The capabilities of the ITER ELM control coil system to achieve the normalised magnetic field perturbation requirements leading to the elimination of Type I ELMs in DIII-D ITER-like plasmas [17] have been evaluated for a range of plasma scenarios and phases among the currents in the three coil rows, including cases in which coils cannot be used due to malfunction [11]. This evaluation has been carried out in the vacuum approximation, i.e. by the linear superposition of the plasma magnetic field and the field from the coils unmodified by the plasma. However, both in ITER and in present experiments the plasma is expected to modify the field that the coils create inside the plasma. The development of a physics criterion for ELM suppression including this effect, and the modelling of the plasma response itself for ITER plasmas in toroidal geometry, remain a subject of R&D and will be taken into account in future studies to refine the results presented below. It is important to note that, given the low resistivity of ITER plasmas, a larger shielding of the resonant field created by the coils could be expected in ITER compared to present devices; which could be somewhat compensated by the different rotation profile (lower toroidal rotation is expected in ITER) [18]. This could decrease the margins in ELM coil current (with respect to the maximum 90 kA-turns) required to achieve a given level of edge magnetic field perturbation for ELM suppression as estimated for ITER following the vacuum approximation.

The empirical criterion used to evaluate the ITER ELM control coil system performance is based on a similar physics argument to its original formulation [17] (i.e. the need for a minimum width for a stochastic layer at the plasma edge by the overlap of magnetic island created by the external perturbation) but has been refined to incorporate the multiple toroidal harmonics which are generated by the ELM control coils [11]. An evaluation of the coil current required to achieve the abovementioned empirical criterion [11] by applying currents in the ITER ELM control coils with a cosine toroidal waveform with $n=4$ and $n=3$ symmetry is shown in Figs. 5.a and 5.b. Since it is not possible to produce a pure $n=4$ waveform with 9 coils, the edge island structure created in such configuration is more complex than expected from a pure $n=4$ perturbation and contains higher n harmonics. These higher n harmonics contribute to closing the gaps between islands allowing the achievement of the empirical ergodization criterion at a lower current in the coils than when a $n=3$ waveform. On the other hand, for this same reason of the $n=4$ waveform containing significant side harmonics, it is likely to lead to more toroidally asymmetric power/particle fluxes at the divertor (see below). In addition, it is expected that higher n harmonics will be more effectively shielded by the plasma [18], so that the advantage, in terms of required current in the coils, of using an $n = 3$ or $n = 4$ waveform for ELM control in ITER remain to be determined once a physics-based criterion for ELM suppression that includes plasma response effects has been developed. Increasing the current above the required minimum value increases not only the width of the

ergodic layer but also the range of relative toroidal phasings between the upper-middle-lower rows of ELM control coils which can meet the ELM suppression criterion. This relaxes the need for alignment between the edge magnetic field and the perturbation applied, which is required to be very precise for the lowest coil current levels required to meet the empirical criterion. Such alignment could be difficult to maintain during phases of the ITER discharges in which the current increases or decreases at fixed magnetic field (i.e. ramp-up or ramp-down in H-mode).

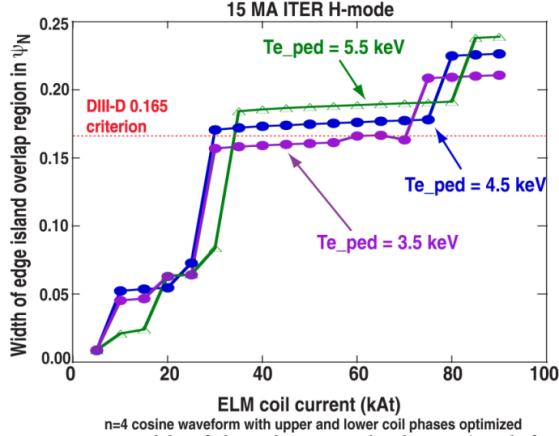


Figure 5.a. Width of the edge ergodic layer (as defined by the island overlap region) in normalised poloidal magnetic flux versus maximum coil current for a current waveform with $n=4$ toroidal symmetry.

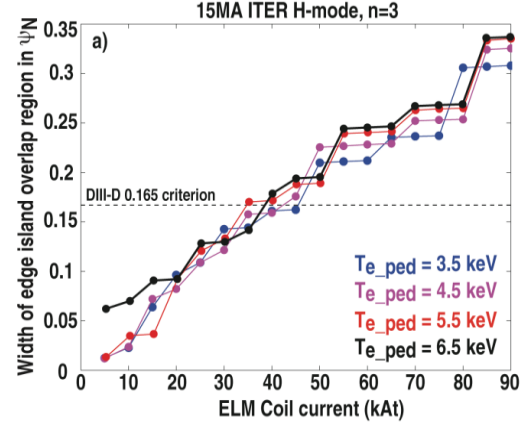


Figure 5.b. Width of the edge ergodic layer (as defined by the island overlap region) in normalised poloidal magnetic flux versus maximum coil current for a current waveform with $n=3$ toroidal symmetry.

This flexibility in the ITER ELM control system allows maintaining the system's performance (as evaluated by the empirical criterion) in case of malfunction of some of the in-vessel coils. Evaluations carried out for the 15 MA scenario show that for the case in which 5 of the equatorial coils are not used, operation with a maximum current of 70 kA-turns in the remaining 22 coils should produce a similar width of the ergodised layer and operational space (in terms of perturbation alignment) than that achieved with all the 27 coils operational with a maximum current of 50 kA-turns. Studies for a range of ITER scenarios, including lower current H-mode operation expected in the initial H/He phase, shows that for $n=3$ perturbations the coil current required to meet the empirical criterion scales in first order linearly with plasma current [11]. Small deviations from this rule are associated with changes at the edge magnetic shear due to the pedestal pressure gradient affecting the bootstrap current and operation at higher q_{95} (i.e. lower current at maximum toroidal field).

The toroidal asymmetries of the power and particle fluxes to ITER PFCs associated with the application of these coils have been evaluated by EMC3-Eierene modelling [12]. This code has also been applied to model toroidally asymmetric fluxes in DIII-D [19] and ASDEX-Upgrade [20]. The perturbation created by the ELM control coils in ITER leads to the splitting of the power flux at the divertor and to toroidally asymmetric deposition away from the separatrix, which resemble the plots of the connection length of the field lines at the plasma edge revealing the well-known homoclinic tangles [21] (see Fig. 6.a and 6.b for $n=4$ and $n=3$ perturbations respectively and Fig. 6.b and 6.c for a comparison of the power flux structure and the connection length with $n=3$). This widens the region over which the high power flux is deposited at the divertor as shown in Fig 6.c for a worst possible case with 100 MW SOL power flow in ITER and no divertor radiation (peak divertor flux of $\sim 10 \text{ MWm}^{-2}$) which would lead to a peak heat flux at the divertor of $\sim 24 \text{ MWm}^{-2}$ in the absence of ELM control coil perturbation. In this respect, the use of an $n=3$ perturbation symmetry with a system of 9 coils per row in ITER instead of $n=4$, is advantageous with regards to getting a more symmetric distribution of footprints in the toroidal direction as shown in Fig. 6.c. It has to be pointed out that the simulations carried out so far indicate that this level of edge ergodization, as estimated in the vacuum approximation, corresponding to the large strike point splitting in Figs. 6.b and 6.c would cause a large particle loss from the main plasma to the divertor target along the ergodized lines, requiring significant additional fuelling ($\sim \text{few } 10^{22} \text{ s}^{-1}$) by pellets in the outer region of the confined plasma to compensate for such loss, given the low efficiency of gas fuelling in ITER. On the other hand this increased level of particle transport at the edge of the confined plasma is favourable to prevent W contamination

of the main plasma in the absence of Type I ELMs, as demonstrated experimentally in [22]. More details on the particle balance and fuelling requirements associated with the application of ELM control coils in ITER can be found in an accompanying paper [12]. Inclusion of the effects of plasma shielding in these calculations in a simplified way has shown that, for ITER conditions, significant shielding effects are expected for resonant modes with $m \leq 7$, which affects the both the extension of the ergodized zone into the confined plasma region and the radial extent of the divertor lobes. Inclusion of these effects in the EM3C-Eierene modelling decreases the loss of particles from the confined plasma (found in the vacuum calculations) but also decreases the spreading of the divertor power flux by the application of the coils. Thus for cases with no divertor radiation, the peak divertor flux is $\sim 17 \text{ MWm}^{-2}$ which corresponds to a reduction of the peak heat flux (when shielding is included) by a factor of ~ 1.5 compared to conditions without current in the ELM control coils; this is smaller than the factor of ~ 2.5 reduction found for calculations done for the vacuum approximation (i.e. no plasma shielding). More details on the modelled power and particle fluxes at the ITER for a range of scenarios and divertor conditions (including high divertor radiation) can be found in [12]. The existence of toroidally asymmetric power and particle flux structures at the divertor could potentially lead to localised erosion areas due to the large particle fluences expected at the ITER divertor. In order to smooth them out, the possibility of rotating the ELM control coil perturbation is being considered in ITER. In such case, it is important to avoid thermal cycling of the W/Cu interface in the divertor PFCs in the areas where the divertor power flux is not toroidally symmetric. To ensure sufficient lifetime of these components, the frequency of rotation of the ELM coil perturbation has been evaluated a function of peak heat flux in the lobes to ensure that the temperature at the W/Cu interface changes by less than 10% through the rotation. Modelling of the heat flux diffusion into the divertor PFC, taking as input the EM3C-Eierene results, has shown that a rotation of the complete power flux pattern with a frequency of $\sim 1 \text{ Hz}$ (corresponding to a frequency of the currents in the coils of 4 Hz ($n=4$)) is sufficient to achieve this goal even for the most conservative case in which the power splitting among lobes would be very asymmetric and the peak power flux in the dominant lobe with $n = 4$ would reach the 20 MWm^{-2} level. For a more realistic case with a peak power of 10 MWm^{-2} and similar peak power flux in all lobes a rotation frequency of the complete heat flux pattern of $1/3 \text{ Hz}$ (corresponding to a frequency of the currents in the coils of 1.0 Hz ($n=3$)) is sufficient.

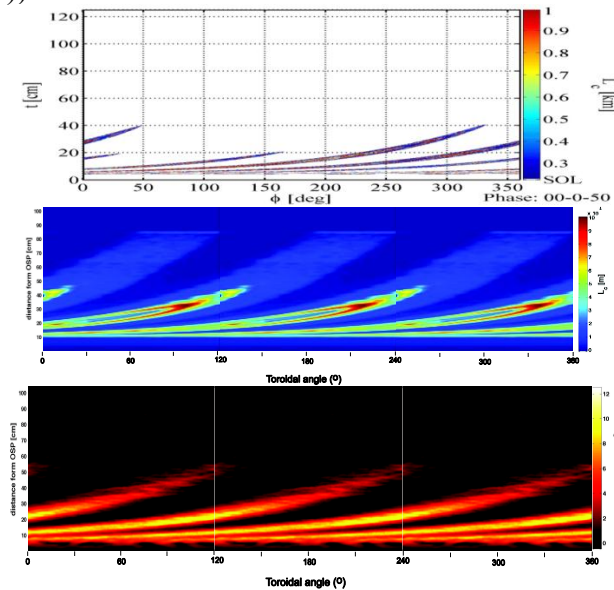


Figure 6.a (top) Connection length of the field lines arriving at the outer divertor target in ITER for a perturbation with $n=4$ symmetry and 90 kA maximum current in the ELM control coils. 6.b (middle) Connection length of the field lines arriving at the outer divertor target in ITER for a perturbation with $n=3$ symmetry and 90 kA maximum current in the ELM control coils. 6.c. Outer divertor power flux for an edge power flux $P_{\text{SOL}} = 100 \text{ MW}$ with no divertor radiation and an ELM coil perturbation as in 6.b.

5. Use of the vertical plasma movements for ELM control in ITER.

Periodic vertical movements of the plasma have been used to trigger ELMs in a number of tokamaks and could be possible in ITER by the use of the in-vessel vertical stabilization coils. A previous evaluation [2] had shown that the potential of this technique for ELM control in 15 MA $Q_{\text{DT}} = 10$ plasmas is very small. A new assessment has been carried out concentrating on its use at lower plasma currents, in view of the possible need to control ELMs during initial H-mode operation to avoid W accumulation. In such case, the achievable peak to peak plasma vertical displacement (limited by the maximum current in the coils and by their ohmic heating) can reach values within the range for

which ELMs have been triggered in several tokamak experiments ($\Delta Z/R \sim (1.0-1.6) 10^{-2}$ [2] and maximum frequencies in the range of 20 - 30 Hz are feasible (limited by the voltage that can be applied to the coils) as shown in Fig 7. These controlled ELM frequencies are above those expected to be required to avoid W accumulation in low current H-mode plasmas (Fig. 2.b). The major uncertainty that remains with regards to the application of this technique at ITER is the development of a physics-based criterion for ELM triggering with this technique; in particular, to determine if ELM triggering requires a minimum plasma displacement (i.e. plasma deformation) and/or a minimum velocity (i.e. induced edge current). This will allow determining whether the achievable vertical displacements and the associated plasma velocities are sufficient to trigger ELMs in ITER or not. In this respect, it is important to note that if the controlled ELMs are triggered by induced edge currents, the high ITER edge temperatures would result in large plasma current densities being induced at the edge by plasma movements, as the expected level of induced current (compared to the plasma bootstrap current in collisionless conditions) scales as :

$$\frac{j_{induced}}{j_{bootstrap}} \sim \frac{T_{ped}^{3/2} \Delta_{ped}^2 v_z^2}{R \beta_{ped}}$$

where T_{ped} , Δ_{ped} , and β_{ped} are the pedestal temperature, width and poloidal beta respectively, R is the major radius of the device and v_z is the plasma vertical velocity. This favours the achievement of large induced currents (in a range similar to that expected in present experiments) in ITER despite the lower plasma oscillation velocities achievable ($v_z \sim 4 \text{ ms}^{-1}$). It is also important to note that, in the event of problems, the recovery of the plasma vertical position control for a displacement of $\sim 5 \text{ cm}$ from the initial magnetic axis for a $\sim 7.5 \text{ MA}$ H-mode is not challenging for the ITER VS system, which is designed to recover a $\sim 16 \text{ cm}$ displacement for a 15 MA L-mode plasma.

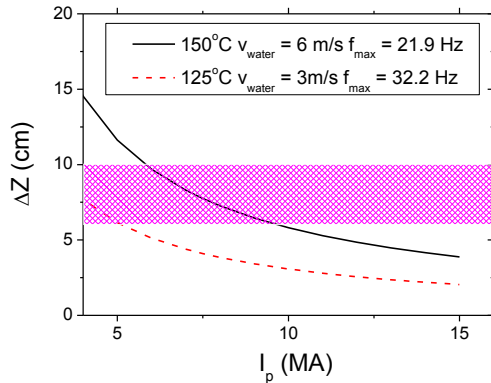


Figure 7. Achievable peak to peak plasma displacement with the ITER in-vessel vertical stabilization coils versus plasma current for ITER H-modes. Two assumptions regarding the maximum temperature allowed in the exit cooling water and on the speed of the cooling water are considered.

Disclaimer : the views and opinions expressed herein do not necessarily reflect those of the ITER Organization.

7. References

- [1] Campbell, D. et al., paper ITR/P1-18, this conference.
- [2] Loarte, A., et al., Proc. 23rd Fusion Energy Conference, Daejeon, South Korea. Paper ITR/1-4.
- [3] Eich, T., et al., J. Nuc. Mat. **415** (2011) S856.
- [4] Jakubowski, M.W., et al., Nucl. Fusion **49** (2009) 095013.
- [5] Dux, R., et al., Nucl. Fusion **51** (2011) 053002.
- [6] Bucalossi, J. et al., Proc. 39th EPS Conference, Stockholm, Sweden, 2012. Paper O3.106.
- [7] Krieger, K., et al., J. Nuc. Mat. **415** (2011) S297.
- [8] Höhnle, H., et al., Nucl. Fusion **51** (2011) 083013.
- [9] Huijsmans, G., et al., paper ITR/P1-23, this conference.
- [10] Futatani, S., et al., paper ITR/P1-22, this conference.
- [11] Evans, T., et al., paper ITR/P1-25, this conf.
- [12] Schmitz, O., et al., paper ITR/P1-24, this conference.
- [13] Baylor, L., et al., paper EX/6-2, this conference.
- [14] Wenninger, R.P., et al., Plasma Phys. Control. Fusion **53** (2011) 105002.
- [15] Maruyama, S., et al., paper ITR/P5-24, this conference.
- [16] Daly, E., et al., Proc. 20th TOFE, Nashville, USA, 2012.
- [17] Fenstermacher, M.E., et al., Phys. Plasmas **15** (2008) 056122.
- [18] Becoulet, M., et al., paper TH/2-1, this conference.
- [19] Frerichs, H., et al., Nucl. Fusion **50** (2011) 034004.
- [20] Lunt, T., et al., Nucl. Fusion **52** (2012) 054013.
- [21] Evans, T., et al., J. Phys : Conf. Ser. **7** (2005) 174.
- [22] Suttrop, W., et al., PRL **106** (2011) 225004.

6. Conclusions

Progress on the determination of ELM control requirements for ITER operation from the non-active phase to $Q = 10$ in DT has been described. In addition significant advances have been carried out in the determination of the power flux characteristics for ELMs in ITER, its control by pellet pacing and with in-vessel ELM control coils showing that the implementation schemes is viable for ITER. The use for of the in-vessel coils for vertical stabilization for W accumulation control in the initial ITER operation in H-mode has been evaluated. Outstanding issues to progress in the ITER ELM control area are described.